JCB Article

Capping protein binding to actin in yeast: biochemical mechanism and physiological relevance

Kyoungtae Kim,[1] Atsuko Yamashita,[2] Martin A. Wear,[1] Yuichiro Maéda,[2] and John A. Cooper[1]

[1]Department of Cell Biology and Physiology, Washington University School of Medicine, St. Louis, MO 63110
[2]Laboratory for Structural Biochemistry, RIKEN Harima Institute at SPring-8, Hyogo 679-5148, Japan

The mechanism by which capping protein (CP) binds barbed ends of actin filaments is not understood, and the physiological significance of CP binding to actin is not defined. The CP crystal structure suggests that the COOH-terminal regions of the CP α and β subunits bind to the barbed end. Using purified recombinant mutant yeast CP, we tested this model. CP lacking both COOH-terminal regions did not bind actin. The α COOH-terminal region was more important than that of β. The significance of CP's actin-binding activity in vivo was tested by determining how well CP actin-binding mutants rescued null mutant phenotypes. Rescue correlated well with capping activity, as did localization of CP to actin patches, indicating that capping is a physiological function for CP. Actin filaments of patches appear to be nucleated first, then capped with CP. The binding constants of yeast CP for actin suggest that actin capping in yeast is more dynamic than in vertebrates.

Introduction

In vitro, capping protein (CP) caps the barbed end of the actin filament (Cooper et al., 1999) and is an essential component for the reconstitution of movement powered by actin polymerization (Loisel et al., 1999). CP is expressed in all eukaryotic organisms, from plasmodia to yeasts to mammals. In vivo, CP is important for actin assembly and cell motility (Cooper et al., 1999).

Saccharomyces cerevisiae CP is a stable heterodimer with subunits of M_r 32 (the α subunit, Cap1) and 33.7 (the β subunit, Cap2), each encoded by one gene (Amatruda and Cooper, 1992; Amatruda et al., 1992). CP is located on cortical actin patches in vivo. In CP null mutant cells, actin patches are present, but depolarized (Amatruda and Cooper, 1992; Amatruda et al., 1992). In addition, CP null mutations are synthetic lethal with null mutations in *SAC6*, which encodes fimbrin, another protein of the actin patch (Adams et al., 1993). CP is necessary for the localization of twinfilin to actin patches, through a direct interaction (Palmgren et al., 2001).

The crystal structure of chicken CP inspired a "tentacle" model in which the COOH-terminal regions of each subunit are proposed to extend out to interact with barbed ends of actin filaments (Yamashita et al., 2003). In that structure, the α and β subunits have similar secondary and tertiary structures, giving the molecule a pseudo twofold rotational axis of symmetry. The overall shape resembles a mushroom, with a stalk and cap. A bundle of six anti-parallel α-helices, three from the NH_2 terminus of each subunit, comprise the mushroom stalk. Next are short stretches of β-strand and reverse turns lying to the side of the stalk and under the mushroom cap. The central region of the protein includes a single 10-stranded anti-parallel β-sheet. Atop this β-sheet are two long α-helices, running anti-parallel to each other. Finally, each subunit has a COOH-terminal extension proposed to function as a flexible tentacle, reaching out to interact with the barbed end of the actin filament. Each COOH-terminal region contains a short amphipathic α-helix.

The tentacle model was supported by a structure/function analysis of chicken CP, in which the actin-binding activities of recombinant mutant chicken CPs were tested (Wear et al., 2003). Here, we tested the tentacle model for yeast CP, using a similar approach. We used a structure for yeast CP prepared by homology modeling from the chicken CP structure.

More importantly, we used the resulting CP actin-binding mutants to test the functional significance of the actin-capping activity of CP in vivo. We assayed the function of the mutant CPs in vivo by testing their ability to rescue null phenotypes. We also determined the localization of the

Address correspondence to John A. Cooper, Campus Box 8228, 660 S. Euclid Ave., St. Louis, MO 63110. Tel.: (314) 362-3964. Fax: (314) 362-0098. email: jcooper@cellbiology.wustl.edu

A. Yamashita's present address is Dept. of Biochemistry and Molecular Biophysics, Columbia University, Room 513, Black Building, 650 West 168th St., New York, NY 10032.

Key words: cytoskeleton; cell motility; polymerization; assembly; *Saccharomyces cerevisiae*

Abbreviations used in this paper: CP, capping protein; wt, wild type.

© The Rockefeller University Press, 0021-9525/2004/02/567/14 $8.00

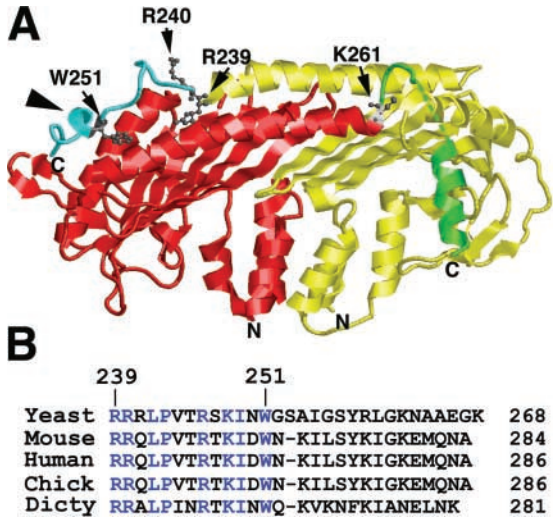

Figure 1. **A model structure for yeast CP.** (A) Cap1 and Cap2 are colored yellow and red, respectively, except that their proposed tentacles are cyan and green, respectively. Certain residues targeted for mutation are indicated. Cap2 residues 268–273 could not be modeled and are indicated as a dashed line. Arrowhead indicates amphipathic α-helix in the COOH-terminal region of the α subunit. (B) Alignment of the COOH-terminal regions of CP α in various species. Residues found in all species are colored blue.

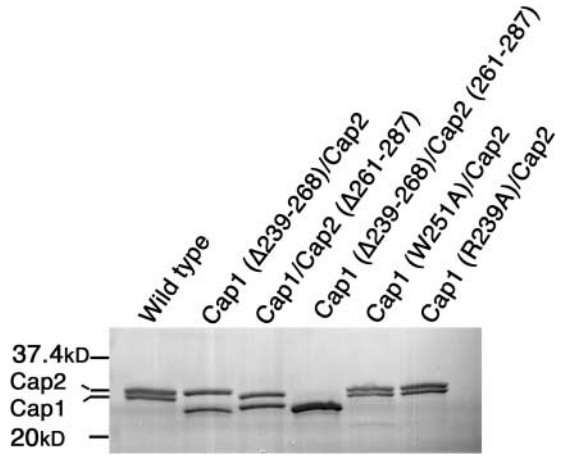

Figure 2. **Purified recombinant CP preparations.** A portion of a 10% SDS–polyacrylamide gel stained with Coomassie Blue is shown. No other bands were present, above or below this region.

mutant CPs in vivo. Actin-capping activity in vitro correlated well with the function and localization of CP in vivo, providing insight into the mechanism of actin assembly and motility along with the function of CP.

Results

A homology model structure for yeast CP

To create a structure for yeast CP, we used SWISS-MODEL (Guex and Peitsch, 1997) to perform homology modeling with the chicken CP structure (Yamashita et al., 2003) as a template. The resulting yeast CP model structure is similar to that of chicken CP, as expected (Fig. 1 A). In particular, the COOH-terminal sequence of each subunit has a short region of amphipathic α-helix as part of the proposed tentacle. At the base of the tentacle are conserved basic residues (Arg239 in Cap1 and Lys261 in Cap2) that may function in tentacle structure or mobility.

Testing the tentacle model

To test the tentacle model, we made mutations in the COOH-terminal regions of each subunit, expressed mutant CP in bacteria, and purified the protein (Fig. 2). To test actin-capping activity, we measured the kinetics of actin polymerization from barbed ends using spectrin-F-actin seeds. For a quantitative comparison of the mutants, binding affinity and kinetic rate constants were determined by modeling the time course of the polymerization reaction. We also measured the effect of mutant CPs on the apparent critical concentration for actin polymerization at steady state. In this assay, capping the barbed end increases the critical concentration to that of the pointed end, producing a plateau, whereas monomer sequestration increases the critical concentration indefinitely. Again, modeling was used to analyze the results quantitatively and to compare the mutant CPs.

First, we measured the capping activity of wild-type (wt) CP (Cap1/Cap2) with yeast and muscle actin. In both cases, CP inhibited actin polymerization nucleated by spectrin-F-actin seeds, and a simple capping model produced good fits (Fig. 3, A and B). From the modeling, the K_d for capping was 1.2 and 3.5 nM for muscle and yeast actin, respectively (Table I). In the critical concentration assay, the K_ds for yeast and muscle actin barbed ends were 4 and 6.25 nM, respectively (see Fig. 5 A, diamond; Fig. 5 B, square; Table I). The on-rate constant (8.9 $\mu M^{-1}s^{-1}$) and off-rate constant ($3.16 \times 10^{-2}s^{-1}$) for CP binding to yeast actin were somewhat higher than those with muscle actin (1.16 $\mu M^{-1}s^{-1}$ and $1.56 \times 10^{-3}s^{-1}$, respectively). Muscle actin was used to test all the CP mutants, and crucial results were confirmed with yeast actin.

Removal of both COOH-terminal regions

The tentacle model predicts that loss of both COOH-terminal regions should cause a complete loss of actin binding. To test this prediction, we expressed and purified a mutant CP lacking the COOH-terminal 30 amino acids of Cap1 (R239-K268) and the COOH-terminal 27 amino acids of Cap2 (K261-L287; Fig. 2). Cap1 R239 and Cap2 K261 are located at the bases of the proposed tentacles in the modeled CP structure (Fig. 1 A). The purified heterodimer, Cap1(Δ239–268)/Cap2(Δ261–287), showed no inhibition of actin polymerization in the seeded actin assembly assay at concentrations up to 75 μM (Fig. 4 A), or in the critical concentration assay at concentrations up to 50 μM (Fig. 5 C, closed circle). The calculated lower limit of the capping K_d was 100 μM. We also tested a mutant with a slightly shorter Cap2 truncation, 24 amino acids, combined with the same Cap1 truncation, Cap1(Δ239–268)/Cap2(Δ264–287). This heterodimer mutant showed a very small effect in the seeded actin assembly assay, with a K_d of 33.4 μM (Table I).

The CP α (Cap1) COOH-terminal region

To test the importance of the proposed Cap1 tentacle in actin capping, we tested a mutant lacking the COOH-terminal 30

Table I. **Binding and rate constants for the interaction of CP mutants and peptides with actin**

CP species	Actin	Critical concentration experiment		Seeded assembly experiment	
		K_d	K_d	k_{+2}	k_{-2}
		nM[a]	*nM*[b]	$\mu M^{-1}s^{-1}$	$s^{-1} \times 10^{-3}$
Wild type	Muscle	4	1.2	1.16	1.56
Wild type	Yeast	6.3	3.5	8.9	31.6
Cap1Δ(239–268)/Cap2	Muscle		10,300	0.00022	2.33
Cap1/Cap2Δ(261–287)	Muscle	25	7.8	2.09	16.3
Cap1/Cap2Δ(261–287)	Yeast	25	17	9.9	168
Cap1/Cap2Δ(264–287)	Muscle	25	8	2.1	17
Cap1Δ(239–268)/Cap2Δ(264–287)	Muscle		33,400	0.00037	12
Cap1 (W251A)/Cap2	Muscle	250	91	0.3	25.9
Cap1 (R239A)/Cap2	Muscle	400	176	0.156	27.5
Cap1 C-30 (peptide)	Muscle		1,710	0.0021	3.6

[a]The value of K_d was determined from the [CP] that changes the critical concentration by 50%, as described in the Materials and methods.
[b]The K_d was calculated from the k_{+2} (On) and k_{-2} (Off) rate constants by modeling the time course of polymerization with reaction 2 (see Materials and methods).

amino acids of Cap1, R239-K268 (Fig. 2). In the seeded assembly assay, Cap1(Δ239–268)/Cap2 inhibited actin polymerization, but only at high concentrations. The data were fit well by a simple capping model (Fig. 4 B). The K_d for capping was 10.3 μM, 8,600-fold greater than that of wt CP (Table I). In the critical concentration assay, the level of F-actin did not change at concentrations of mutant CP up to 25 μM (Fig. 5 B, closed circle). The lower limit for the K_d was 50 μM. Thus, the proposed Cap1 tentacle is very important for capping.

To test whether the Cap1 tentacle alone is sufficient to bind actin, we assayed a synthetic peptide corresponding to the COOH-terminal 30 amino acids of Cap1. The peptide inhibited actin polymerization in the seeded assembly assay. The data were fit well by a model that included both capping and monomer binding, but not by simpler models with only capping or monomer binding (Fig. 4 C). From the modeling, the capping K_d was 1.71 μM, with an on-rate constant of 0.0021 $\mu M^{-1}s^{-1}$ (Table I). For monomer binding, the K_d was 2.86 μM, and the on-rate constant was 0.0084 $\mu M^{-1}s^{-1}$. The peptide had no effect in the critical concentration assay; however, concentrations of peptide >8 μM caused the formation of gross precipitates. Thus, the proposed Cap1 tentacle sequence alone is sufficient to bind actin, and even to cap barbed ends, albeit with low affinity. Circular dichroism analyses of the free peptide showed no secondary structure (unpublished data), so the active actin-binding conformation of the tentacle may be promoted by its connection to the body of the protein.

Point mutations in the Cap1 COOH-terminal region

The proposed tentacle for Cap1 includes an amphipathic α-helix (Fig. 1 A, arrowhead). The hydrophobic side in-

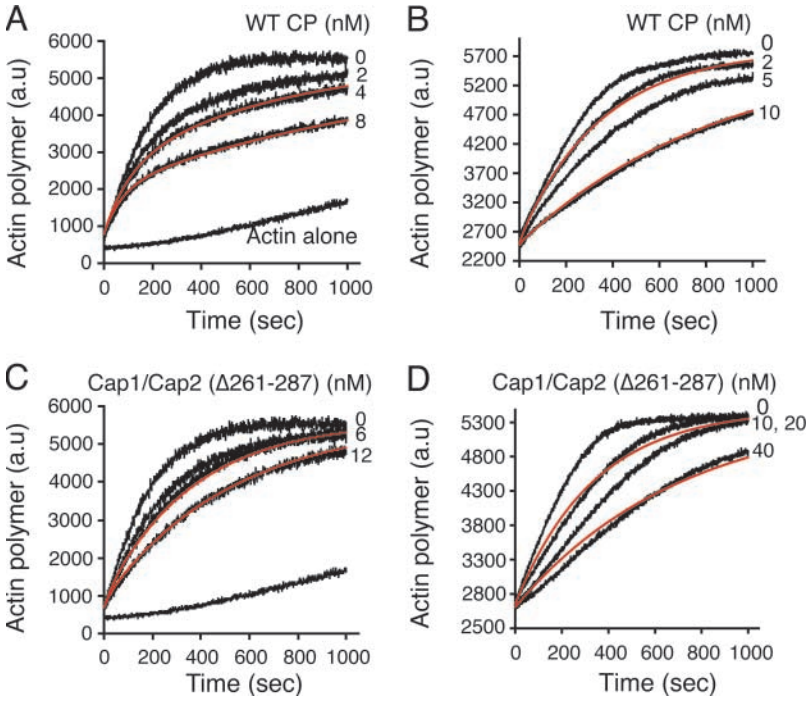

Figure 3. **Effect of CP on seeded actin polymerization: muscle vs. yeast actin.** Experimental and fitted data are in black and red, respectively. (A) WT CP and muscle actin. (B) WT CP and yeast actin. (C) Cap1/Cap2(Δ261–287) and muscle actin. (D) Cap 1/Cap2(Δ261–287) and yeast actin.

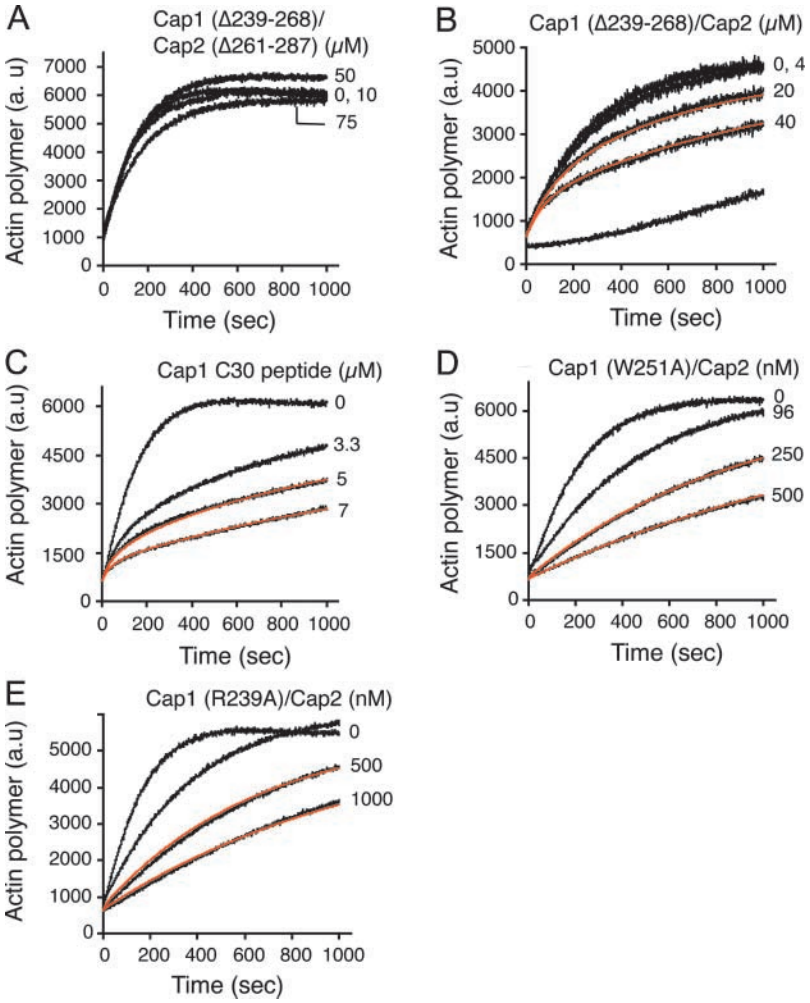

Figure 4. **Effect of CP mutants on seeded actin polymerization.** Experimental and fitted data are in black and red, respectively. (A) Cap1Δ(239–268)/Cap2(Δ261–287). (B) Cap1Δ(239–268)/Cap2. (C) Cap1 C-30, a synthetic peptide corresponding to the Cap1 COOH-terminal 30 residues, 239–268. (D) Cap1 (W251A)/Cap2. (E) Cap1 (R239A)/Cap2.

cludes three highly conserved residues: W251, A254, and I255. W251 is present in the CP α subunit of all species (Fig. 1 B). We replaced W251 with alanine. Purified Cap1(W251A)/Cap2 protein inhibited actin polymerization in the seeded assembly assay (Fig. 4 D). A capping model fit the data well. The K_d for capping was 91 nM, 76-fold less than that of wt CP (Table I). The off-rate constant was increased 17-fold, and the on-rate constant was decreased fourfold. Capping was also seen in the critical concentration assay, where the K_d was 250 nM (Fig. 5 D, triangle; Table

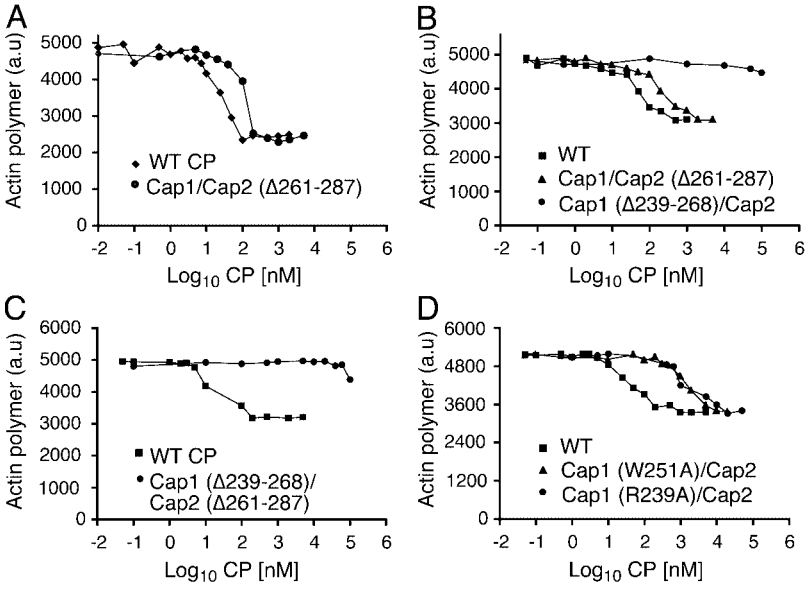

Figure 5. **Effect of CP mutants on the apparent critical concentration for actin polymerization at steady state.** Pyrene actin fluorescence intensity, reflecting polymerized actin, is plotted vs. the log of the CP concentration. CP mutants are as indicated on each panel.

Table II. **Compilation of data on CP function**

Mutation	Actin capping K_d	Actin polarization[a]	Growth in sac6 background[b]	CP localization pattern[c]	CP intensity at patches[d]
wt	1 nM	81 ± 3	+++	Localizes at patches	+++
Cap2 K261A		89 ± 2	+++	wt	+++
Cap2Δ264–287	8 nM	86 ± 2	+++	wt	+++
Cap1 R241A		85 ± 3	+++	wt	+++
Cap1 S257R		83 ± 3	+++	ND	
Cap2Δ261–287		82 ± 3	+++	wt	+++
Cap1 G256R		82 ± 3	+++	ND	
Cap1 G252R		81 ± 3	+++	ND	
Cap1 S253R		80 ± 3	+++	ND	
Cap1 W251F		78 ± 3	+++	wt	+++
Cap1 A254R		76.5 ± 3	+++	wt	+++
Cap1 I255R		74 ± 3	+++	ND	
Cap1 R240A		68 ± 3	+++	wt	+++
Cap1Δ258–268		62 ± 3*	++	wt	+++
Cap1 W251A	91 nM	60 ± 3*	+	Partial	++
Cap1 W251R		46 ± 4*	+	Partial	++
Cap1 R239A	176 nM	39 ± 3*	+	Diffuse	+
Cap1 R239E		7 ± 2*	0	Diffuse	-
Cap1 R240E		5 ± 2*	0	Diffuse	-
Cap1Δ251–268		5 ± 2*	0	Diffuse	-
Cap1Δ239–268	10.3 μM	5 ± 2*	0	Diffuse	-
Cap1 RR239 240AA		4 ± 1*	0	Diffuse	-

Mutations are ranked by their value for actin polarization, with wt at top. Note that the rank order is the same for the other criteria, when values are present.
[a]Percentage of 200 small-budded cells with <4 actin patches in the mother ± SEP (standard error of proportion = sqrt(p*(1 − p)/*n*). Values statistically different ($P < 0.05$) from that of wt are indicated with an asterisk.
[b]Growth of 10-fold serial dilutions, relative to wt. +++ indicates similar to wt. ++ and a + indicate 10- and 100-fold decrease in growth, respectively. 0 is no growth.
[c]The pattern of immunofluorescence staining is listed as wt, diffuse, or partial, corresponding to representative images in Fig. 6. ND, not determined.
[d]The intensity of patch staining in buds is indicated as +++ (bright) to + (dim).

I). Thus, W251 is important for capping. The residue may be important for the structure of the tentacle, or it may interact directly with actin.

The tentacle model predicts that the COOH-terminal regions, the proposed tentacles, are mobile relative to the body of the protein. The tentacle should pivot about its attachment site. R239 is a highly conserved residue at this location (Fig. 1, A and B). To test whether R239 is important for capping, we replaced it with alanine. The Cap1 (R239A)/Cap2 protein inhibited polymerization in the seeded assembly assay (Fig. 4 E). A capping model gave a good fit, and the K_d for capping was 176 nM, 150-fold higher than that of wt (Table I). The on-rate constant was decreased 7.5-fold, and the off-rate constant was increased 18-fold, relative to wt. Capping was also seen in the critical concentration assay, where the K_d was 400 nM (Fig. 5 D, circle; Table I). Thus, the R239A mutation may affect the mobility or structure of the tentacle, such that the tentacle does not properly interact with actin filaments.

The CP β (Cap2) COOH-terminal region

We tested the tentacle model for CP β (Cap2) by removing the COOH-terminal 27 amino acids, K261–L287, which comprises the entire proposed tentacle. In a previous experiment, a 21-aa truncation had normal actin-binding activity, using partially purified protein from yeast and falling ball viscometry (Sizonenko et al., 1996). Here, purified Cap1/Cap2(Δ261–287) inhibited polymerization in the seeded assembly assay, and a capping model fit the data well (Fig. 3 C). With muscle actin, the K_d for capping was 7.8 nM, increased approximately sevenfold from that of wt CP (Table I). The difference was due almost entirely to an increase in the off-rate constant. With yeast actin, the results were similar; the K_d was 17 nM, increased approximately fivefold from that of wt CP (Fig. 3 D, Table I). In the steady-state critical concentration assay, Cap1/Cap2(Δ261–287) exhibited capping activity, with a K_d of 25 nM for both muscle and yeast actin (Fig. 5, A and B; Table I). Increased concentrations, up to 10 μM, did not change the critical concentration further. A shorter truncation of 24 residues produced similar results (Table I, Cap1/Cap2(Δ264–287)). The proposed Cap2 tentacle alone, as a free synthetic peptide and a GST fusion protein, had no actin-binding activity (unpublished data). However, the synthetic peptide showed no evidence of a secondary structure by circular dichroism. This region includes an amphipathic α-helix in the homology model structure, so that feature may be necessary for activity and may only exist when the tentacle is attached to the protein. Overall then, the proposed tentacle of Cap2 is necessary for high affinity capping, but the proposed tentacle of Cap1 is much more important.

Function and localization of CP mutants in vivo

We assayed the ability of a number of CP mutants to function in cells, motivated by two major goals. First, actin cap-

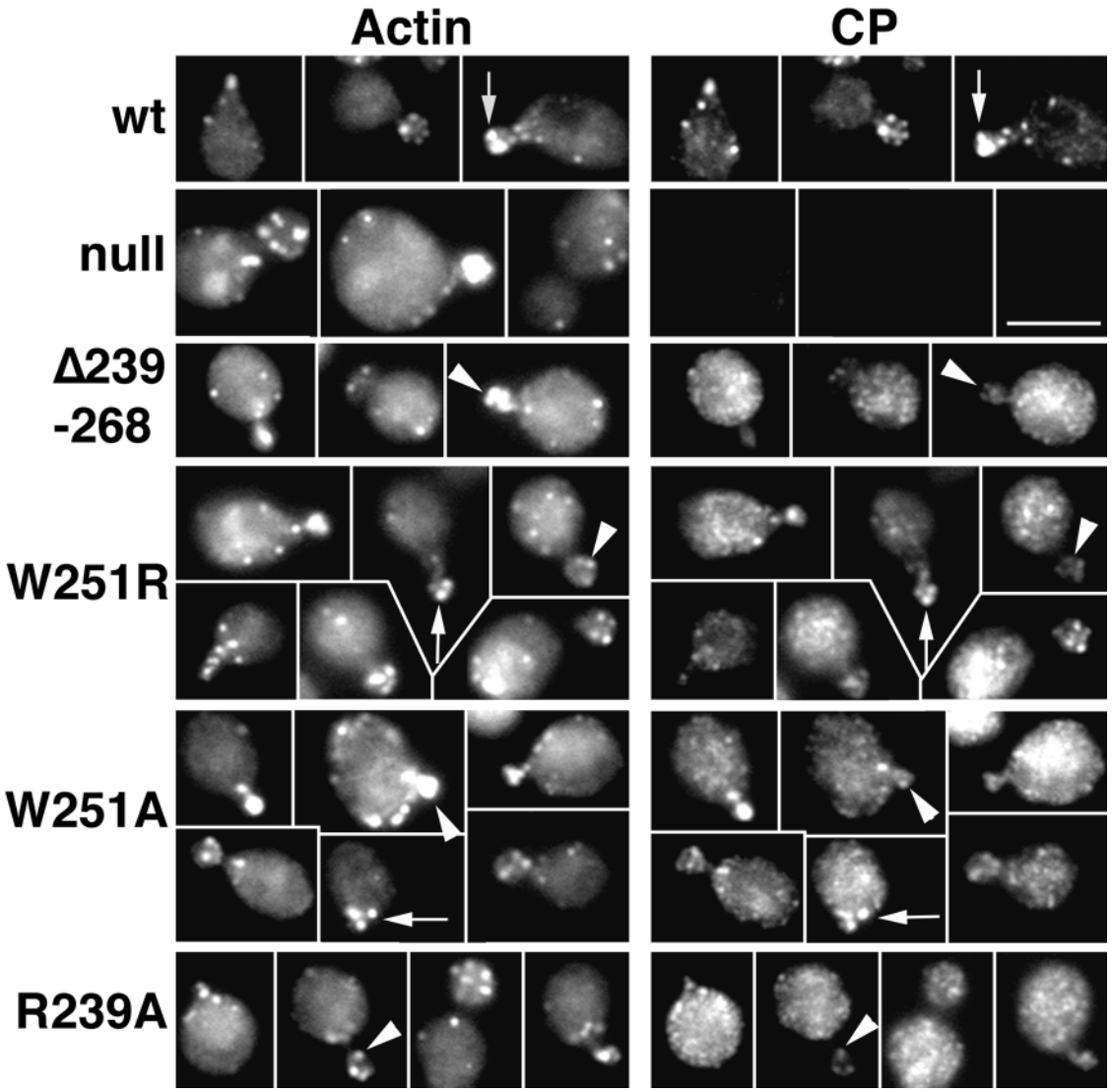

Figure 6. **Localization of F-actin and CP in mutants.** Representative images of the results for key Cap1 mutations, as indicated. Arrows indicate examples of CP colocalization with cortical actin patches; arrowheads indicate examples of colocalization failure. Bar, 5 μm.

ping is hypothesized to be a physiologically relevant function of CP. To test this hypothesis, we asked whether actin capping, as measured biochemically in vitro, correlates with the ability of CP to function normally in vivo. Second, to address the role of capping in the assembly of the actin patch, we determined the localization of these CP mutant proteins in vivo. In the sarcomere of striated muscle, CP (CapZ) appears to bind first to a periodic scaffold, independently of actin. Then, CP may capture or nucleate an actin filament (Schafer et al., 1993, 1995). On the other hand, in the dendritic nucleation model for lamellipodial protrusion in animal cells (Pollard and Borisy, 2003), CP caps older barbed ends after they have formed, which "funnels" actin polymerization to the new ends near the membrane (Carlier and Pantaloni, 1997). We asked which model applies to the yeast actin patch.

To test function in vivo, we first measured the ability of all the CP mutations to rescue two phenotypes characteristic of null mutations—depolarization of the actin cytoskeleton and synthetic lethality with null mutations in the fimbrin gene *SAC6*. The assays consisted of staining cells with rhodamine-phalloidin to reveal the actin distribution and growing strains on plates after plasmid shuffle in a *sac6* background (Table II). Next, CP mutant proteins were localized by anti-CP staining, using rhodamine-phalloidin as a second label to reveal actin patches (Fig. 6).

For CP α, the mutant with deletion of the entire 30-aa tentacle, Cap1Δ239–268, showed no rescue of either null mutant phenotype (Table II). An 18-aa truncation, Cap1Δ251–268, also showed no rescue in either assay, but an 11-aa truncation, Cap1Δ258–268, showed partial rescue in both assays. Regarding localization, CP was diffuse throughout the cytoplasm and was not concentrated at patches in Cap1Δ239–268 and Cap1Δ251–268 cells (Fig. 6, arrowheads), whereas CP localized normally to patches in Cap1Δ258–268 cells (unpublished data).

To assess the importance of the amphipathic α-helical region of the Cap1 tentacle (W251–S257) for function in vivo, we changed single aa residues within that region. The conserved residues Trp251, Ala254, and Ile255 are found

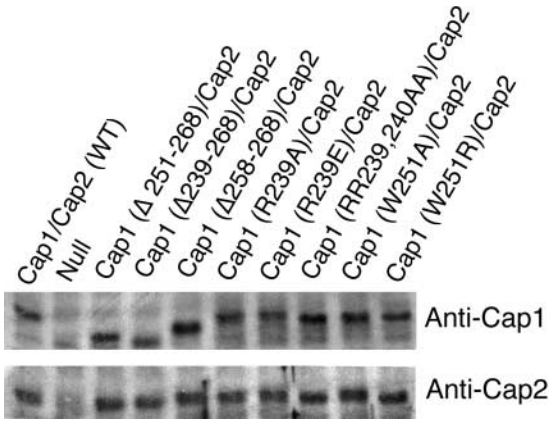

Figure 7. **Immunoblot of CP in whole-cell extracts of yeast mutant strains with decreased CP function in vivo.** The same amount (20 μg, determined by Bradford assay of the cell lysate) of total protein was loaded on a 10% SDS–polyacrylamide gel, blotted, and probed with antibodies against Cap1 or Cap2.

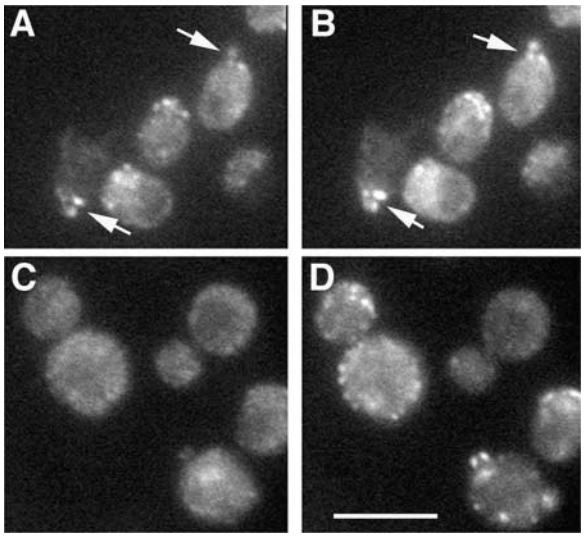

Figure 8. **Twinfilin localization to cortical actin patches in a CP actin-binding mutant.** The localization of twinfilin (A and C) and actin (B and D) was examined in wt (A and B) and Cap1 Δ239–268 (C and D) strains. Bar, 5 μm. Arrows indicate cortical actin patches.

on the hydrophobic side. W251A and W251R mutations produced large (but not complete) loss of function in both assays (Table II). W251F was similar to wt. Changing Ala254 or Ile255 to Arg resulted in wt levels of function in both assays (Table II). We also changed Gly252, Ser253, Gly256, and Ser257 to Arg, one at a time; none of the mutations showed any difference compared with wt. Thus, W251 is the only residue in the helical domain necessary for CP function in vivo. CP localization in the W251A and W251R strains showed decreased intensity of patch staining with increased diffuse cytoplasmic staining (Fig. 6).

We tested the importance of three residues near the proposed pivot point of the Cap1 tentacle: Arg239, Arg240, and Arg241 (Fig. 1 B). Residues Arg 240 and Arg 241 are located on the surface of the protein, with their side chains exposed to solvent (Fig. 1 A; only Arg240 was indicated). The side chain of Arg239 is oriented toward the body of the protein, and Arg239 makes close contacts with surrounding residues. Thus, Arg239 may anchor the tentacle and be necessary for pivoting. An R239A mutation produced severe loss of function in both assays, whereas R240A and R241A mutations had no effect (Table II). A double mutant, RR239 240AA, showed complete loss of function, as did the single change of charge mutations R239E and R240E (Table II). CP was localized normally in R240A and R241A strains. The R239A mutant showed increased diffuse staining as well as patch localization; the patch staining intensity was much less than that of wt (Fig. 6). RR239 240AA, R239E, and R240E showed diffuse CP staining (Table II).

For CP β, we truncated the entire proposed tentacle by introducing a stop site that removed 27 residues, creating Cap2Δ261–287. The mutation provided complete rescue of both null mutant phenotypes (Table II). The localization of this mutant CP was normal. A shorter truncation, Cap2Δ264–287, produced similar results, as did the point mutation Cap2 K261A.

When a mutation produced loss of function in vivo, we asked whether the level of the mutant CP was normal, to consider loss of protein as a trivial explanation for loss of function. By immunoblots, both CP subunits were expressed at approximately normal levels in all CP mutants with any loss of function (Fig. 7).

Additional tests of CP function in vivo

To address the question of whether the actin-binding activity of CP is necessary for all its functions in vivo, we compared the phenotype of a CP actin-binding mutant with that of a null mutant in four additional assays.

First, twinfilin is located at the actin patch and binds directly to CP (Palmgren et al., 2001). In CP null mutants, twinfilin localization at patches is greatly decreased (Palmgren et al., 2001). Here, we found that twinfilin localization to actin patches in Cap1Δ239–268 was also greatly decreased (Fig. 8).

Second, we assayed addition of rhodamine-actin to permeabilized cells, which is increased in CP null mutants (Li et al., 1995). The Cap1Δ239–268 mutant showed increased addition of rhodamine actin, similar to that in a *cap1* null mutant. We added 0.5 μM exogenous rhodamine-actin to permeabilized cells. Levels of rhodamine-actin assembly were quantified by averaging fluorescence intensities from buds of small-budded cells. For Cap1Δ239–268, the level was 1.7 times that of wt, and *cap1*Δ was 2.2 times that of wt (Fig. 9 A). We also graphed the rhodamine fluorescence intensities as a histogram for both whole buds (Fig. 9 B) and individual patches (Fig. 9 C). The distribution of fluorescence intensities was higher in both *cap1* mutants, relative to that of wt, for both whole buds and individual patches. The two mutants were similar to each other.

Loss of CP function might increase the number of barbed ends, and added rhodamine-actin may polymerize at free barbed ends. In the assay, rhodamine-actin is present at a concentration greater than the barbed end critical concentration and near that of the pointed end. To determine how much of the rhodamine-actin addition here was caused by free barbed ends, we added purified CP at 500 nM to the permeabilized cells before adding rhodamine-actin. CP treatments in the

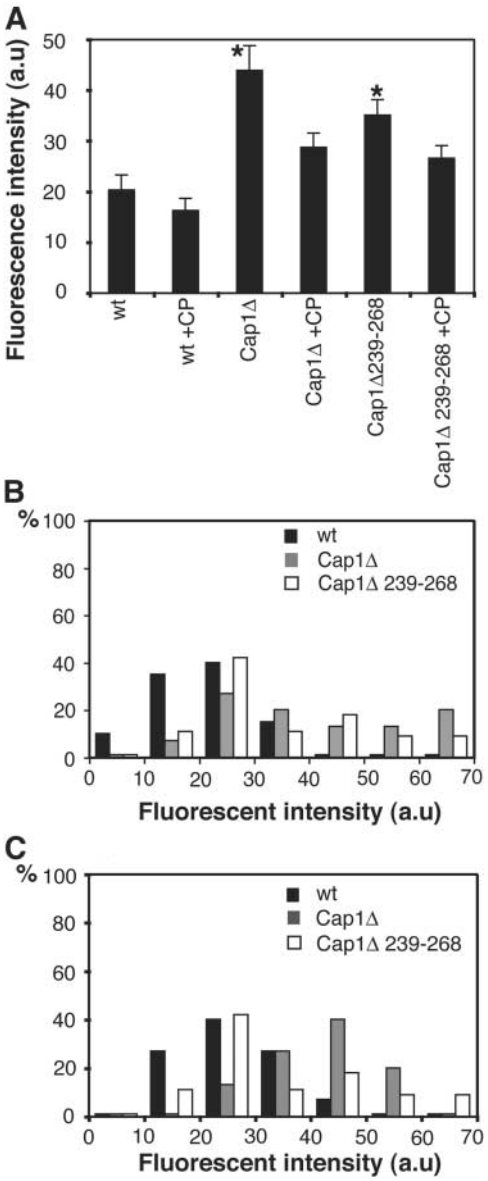

Figure 9. **Rhodamine-actin incorporation into permeabilized cells.** 0.5 μM rhodamine-actin was added to permeabilized cells for 10 min. Small-budded cells were viewed by fluorescence microscopy. (A) The mean intensity of fluorescence associated with the entire bud was quantified. The error bar is SEM. Asterisks mark cases where the difference between the mutant and wt is statistically significant ($P < 0.05$). B and C are histograms of the intensity of fluorescence of the entire bud (B) and of individual patches in the bud (C). The unit of fluorescence intensity is arbitrary.

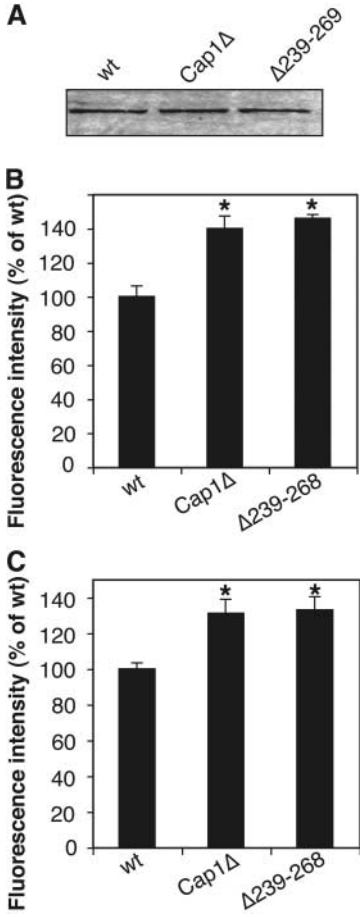

Figure 10. **Quantitation of actin in CP mutants.** (A) Immunoblot of actin in whole-cell extracts of yeast strains. The same amount (20 μg) of total protein was loaded. (B) Bars represent the mean value of bound rhodamine-phalloidin fluorescence for a cell population measured in a fluorometer. The values for each strain were normalized for total protein content, and wt was set at 100%. (C) Bars represent the mean value of bound rhodamine-phalloidin fluorescence measured for individual cells in a fluorescence microscope. The error bar is SEM. Asterisks marks cases where the difference between the mutant and wt is statistically significant ($P < 0.05$).

two *cap1* mutant strains decreased the level of actin incorporation by a significant amount, but not to the level of a control wt strain without CP (Fig. 9 A). For wt cells, CP treatment also decreased the amount of actin incorporation, but only by a small amount. Thus, the *cap1* mutants do appear to have increased numbers of free barbed ends, and the actin-binding mutant was similar to the null mutant.

Next, we measured the levels of total actin and F-actin. By immunoblot, the level of total actin was the same in wt, CP null, and CP actin-binding mutant cells (Fig. 10 A). We measured F-actin by rhodamine-phalloidin binding assays, examining either a population of cells with a fluorometer or individual cells with a fluorescence microscope. Under both methods, the level of F-actin in both mutants was increased by similar amounts. By fluorometry, the level was ~1.4 times that of wt (Fig. 10 B), and by microscopy, the level was ~1.3 times that of wt (Fig. 10 C). These results differ from a previous result from our lab (Karpova et al., 1995), where the F-actin level as measured by fluorometry and rhodamine-phalloidin binding went down. As part of this paper, we repeated those experiments carefully, and we also used fluorescence microscopy as an independent approach. We do not have a good understanding of the basis for the discrepancy. Combined with the previous result that the CP mutants had increased numbers of free barbed ends, the increase in F-actin implies that the actin monomer concentration is greater than the barbed end critical concentration, which is consistent with our understanding of actin assembly in general.

Finally, we measured the motility of cortical actin patches. We used Sac6-GFP to label the patches, collected movies of

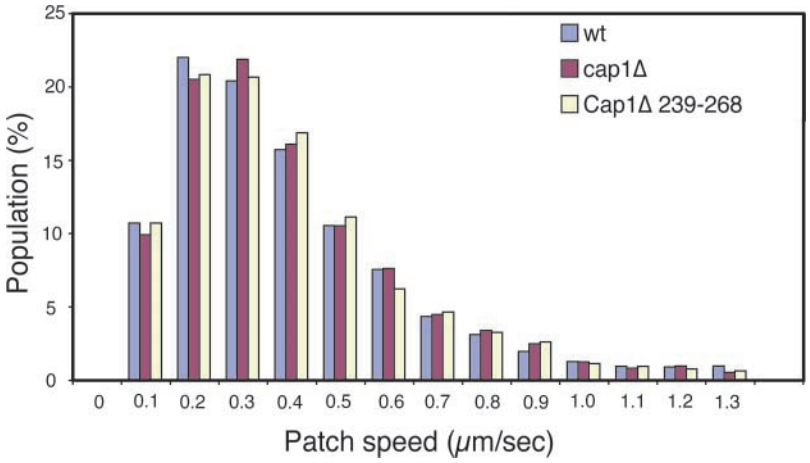

Figure 11. **Histogram of speeds of actin patches moving in CP mutants and wt.** The percentage of the population is plotted vs. patch speed (μm/s).

patches, and tracked the patches with the assistance of computer software. The speed of the patches was very similar in wt, *cap1*Δ, and Cap1Δ239–268 strains (Fig. 11; 0.1–1.3 μm/s). To analyze the motion of the patches further, we plotted the mean squared distance against time for all the tracks. For all three strains the plots were linear, indicating that the motion is largely random, and the slopes of the linear portions were similar, confirming that the speeds are similar (unpublished data).

Discussion

In this paper, we have defined the structural basis for actin capping by CP, and we have used this information to provide evidence that actin capping is the major physiological function of CP, sufficient to account for all null mutant phenotypes. Also, actin capping is necessary for the localization of CP to actin patches, consistent with the dendritic nucleation model for actin assembly (Pollard and Borisy, 2003).

The tentacle model for CP binding to actin

An atomic structure for chicken CP was recently solved using x-ray crystallography (Yamashita et al., 2003). In the chicken CP structure, the COOH-terminal region of the α subunit is largely exposed to solvent, but is folded down onto the surface of the protein with an apparent hydrophobic interaction between the body and the COOH-terminal region. In contrast, the COOH-terminal region of the CP β subunit is extended, lacking any interactions with the body of the protein. These features, coupled with the symmetry of the barbed end of the actin filament, inspired a tentacle model in which the COOH-terminal regions are mobile, extend out from the body of the protein, and bind to the barbed end (Yamashita et al., 2003). The actin-binding aspect of this model was supported by experiments with chicken CP (Wear et al., 2003).

CP is highly conserved, so we constructed a homology model for yeast CP based on the chicken structure. We tested the actin-binding aspect of the tentacle model by deleting the proposed tentacles and measuring actin-capping activity in vitro. Loss of both COOH-terminal regions caused a complete loss of actin-binding activity. Loss of the α COOH-terminal region caused a large decrease in actin-capping activity (8,600-fold), and loss of the β COOH-terminal region caused a small decrease in actin-capping activity (eightfold). Single amino acid changes confirmed the primary importance of the α COOH-terminal region, and demonstrated the importance of residues on the hydrophobic side of an amphipathic helix in the region and at a potential pivot point where the proposed tentacle meets the body of the protein. The proposed α tentacle alone, as a synthetic peptide, displayed actin-capping and monomer-binding activities, although they were weak. Based on the observation that a single COOH-terminal region, either free or attached to CP, is able to cap, we suggest that the COOH-terminal regions bind to interfaces between actin subunits in the filament, as discussed previously (Wear et al., 2003).

These results test and confirm the actin-binding aspect of the tentacle model, but the experiments do not test the prediction that the COOH-terminal regions are mobile and extend away from the body of CP to bind the barbed end. Indeed, recent analyses of the interaction of S100 protein with chicken CP suggest that the COOH-terminal region of CP α is not extended (Wear and Cooper, 2004).

Physiological function and localization of CP

We used these actin-binding mutants to test two hypotheses—that CP's major physiological function is to bind actin, and that CP is present at cortical actin patches because it binds actin. We found that CP actin-binding mutants had the same phenotype as CP null mutants for every phenotype assayed—polarization of the actin cytoskeleton, synthetic lethality with *sac6*, twinfilin localization, incorporation of rhodamine-actin into permeabilized cells, levels of F-actin and total actin, and actin patch motility. Together, these results show that CP's actin-capping activity is necessary for CP to function in vivo. CP does possess other biochemical activities, such as binding twinfilin (Palmgren et al., 2001), and those may also be important for function in vivo. The results here do not argue against that possibility, which we see as likely.

We also localized the CP actin-binding mutant proteins in vivo, performing a double localization with actin patches. The order of severity of the mutations for loss of actin binding in vitro was essentially the same as the order of severity for loss of function in vivo and for localization to actin

patches (Table II). The results suggest that actin filaments with free barbed ends are formed first and are then capped by CP, which agrees with the hypothesis that actin filaments with free barbed ends are nucleated by the action of Arp2/3 complex (Machesky and Gould, 1999; Pollard and Borisy, 2003). Actin patches are still present in CP null mutants (Amatruda et al., 1990), also consistent with CP localization being "downstream" of actin assembly.

One interesting aspect of these results was how much of a defect in CP's actin-capping activity was compatible with apparently normal function and localization—at least 10-fold. One interpretation of this result is that the cell contains a 10-fold excess of CP, so that actin filaments are still capped in adequate numbers and with adequate speed for viability and growth in these CP mutants.

Comparison of yeast and chicken CP results

A recent analysis of actin-binding mutations for chicken CP had results qualitatively similar to those here for yeast CP (Wear et al., 2003). Loss of both COOH-terminal regions produced a complete loss of actin binding, and the α COOH terminus was more important than the β COOH terminus. Previous experiments, performed without the benefit of the CP crystal structure or bacterial expression system, suggested that yeast and chicken CP might bind actin differently (Hug et al., 1992; Sizonenko et al., 1996). Our current analysis shows that this is not the case. The high degree of sequence conservation among CP subunits from various eukaryotes suggests that this model for binding actin may apply to other CPs. Indeed, nematode CP can function in yeast, rescuing null mutant phenotypes (Waddle et al., 1993).

Implications of the biochemical results for actin assembly in vivo

One interesting and potentially important difference between yeast and chicken CP is that yeast CP binds actin less well than does chicken CP, by a factor of ~10 in K_d. This difference holds for actin from yeast as well as from muscle. Moreover, the off-rate constant for the dissociation of yeast CP from the actin filament is higher than that of chicken CP by a factor of 10 or more. Therefore, the half-life of a capped actin filament in yeast should be 22 s, compared with 30 min in vertebrates (Schafer et al., 1996).

One can also calculate the expected half-life of a free barbed end, and how much that barbed end should grow before being capped. We confirmed previous values for cellular content of actin and CP in yeast (Amatruda and Cooper, 1992; Nefsky and Bretscher, 1992; Karpova et al., 1995). The total concentration of actin in the cytoplasm is 5.3 μM, and the total concentration of CP is 1.3 μM (see Materials and methods). To estimate the half-life of a new free barbed end until the time when it is bound by CP, one must assume a value for the concentration of free cytoplasmic CP. Most CP appears to be localized at patches in images of wt cells (Fig. 6; Amatruda and Cooper, 1992), and the localization results here indicate that CP found at patches is indeed bound to actin. Thus, one might estimate the free CP cytoplasmic concentration at 10% of the total, or 0.13 μM. With the on-rate constant of 9 $\mu M^{-1}\ s^{-1}$ for yeast CP and yeast actin (Table I), the rate of capping is 9 $\mu M^{-1}\ s^{-1} \times 0.13\ \mu M = 1.17\ s^{-1}$, which converts to a half-life of 0.4 s. The total actin concentration is 5.3 μM, and a conservative estimate of the actin monomer concentration might be 0.5 μM, near the critical concentration for the pointed end. At an actin monomer concentration of 0.5 μM, a free barbed end would grow by two subunits, given the actin elongation rate constants and the half-life of 0.4 s. This value of two subunits is probably a lower limit. The actin monomer concentration may be higher if pointed ends are capped by Arp2/3 complex. Also, the effective actin monomer concentration in the patch may be higher if proteins that bind monomer in the patch are able to "deliver" that monomer to a free barbed end. Even so, this analysis suggests that actin filaments of patches are short, which agrees with the size of patches (Mulholland et al., 1994). Actin cables of yeast presumably contain longer actin filaments, bundled together, which were nucleated by formins. Formins remain with the barbed end of the nucleated filament and protect it from capping by capping protein (Zigmond et al., 2003), which may account for the increased filament length in cables versus patches.

The results here also address the question of how the dendritic nucleation model (Pollard and Borisy, 2003) applies to actin patch assembly and motility, especially the funneling model for CP's role in dendritic nucleation (Carlier and Pantaloni, 1997). Previous papers showed that Arp2/3 complex and cofilin activity are important for actin patch assembly and motility (Lappalainen and Drubin, 1997; Winter et al., 1997; Idrissi et al., 2002), and that actin polymerization is important for patch movement (Carlsson et al., 2002). These findings are in accord with the dendritic nucleation model. Here, we found that the loss of CP's actin-capping activity led to an increase in free barbed ends per patch and per small bud, based on addition of rhodamine-actin to permeabilized cells. This result is also predicted by the dendritic nucleation model.

The funneling model for CP's role in dendritic nucleation predicts that the absence of CP should cause decreased assembly and motility at the locations of Arp2/3-induced nucleation, secondary to increased actin assembly at other locations of barbed ends in the cell. Here, CP actin-binding and null mutants showed an increase in the level of F-actin per cell and per bud, based on rhodamine-phalloidin binding, in agreement with the funneling model. However, CP actin-binding and null mutants showed no change in actin patch motility, based on measurements of individual patch speed, which runs counter to the model. One potential explanation for this result is that yeast cells may not have a substantial pool of barbed ends in the cytoplasm in general, outside of patches and perhaps cable ends, and thus do not need CP to cap those ends to keep the actin monomer concentration high enough to support actin assembly at patches. Another possibility is that some other factor caps barbed ends. Aip1 has been reported to cap barbed ends as a complex with cofilin (Cof1) in *Xenopus* and *Saccharomyces* (Okada et al., 2002; Balcer et al., 2003); however, an *aip1 cap2* double-null mutant shows only a minimal synthetic effect in terms of growth (Rodal et al., 1999). Biochemical and sequence analyses have not revealed any other types of barbed end capping proteins, such as gelsolins, in *Saccharomyces*.

Materials and methods

Chemicals and reagents were from Fisher Scientific and Sigma-Aldrich, unless stated otherwise. Synthetic peptides corresponding to the COOH-terminal 30 aa and 28 aa of yeast Cap1 and Cap2, called Cap1 C-30 and Cap2 C-28, respectively, were obtained from Biomolecules Midwest. They were purified by reverse-phase HPLC, and their sequence was verified by electrospray mass spectrometry.

Oligonucleotide primers are listed in Table III, CP mutant plasmids in Table IV, and yeast strains in Table V. Oligonucleotide-mediated site-directed mutagenesis was performed using the QuikChange® Site-Directed Mutagenesis Kit (Stratagene). Mutations were verified by DNA sequencing.

Homology modeling of yeast CP

The three-dimensional model of yeast CP was built with SWISS-MODEL (Guex and Peitsch, 1997). Cap1 was built by providing the Cap1 sequence (Swiss-Prot: P28945) with the coordinates of the chicken CP α subunit (PDB code: 1IZN) as a template; Cap2 by providing the Cap2 sequence (Swiss-Prot: P13517) with the coordinates of the chicken CP β1 subunit. Residues 268 to the COOH terminus of Cap2 were not modeled by SWISS-MODEL because the sequence homology with the chicken CP β subunit in this region is fairly low. Residues 268–273 of Cap2 are missing in the yeast CP homology model because they reside in a loop region and could not be modeled manually. Structures for the residues 274–287 of Cap2 were built by manually replacing the residues of chicken β1 with those of yeast Cap2 using the graphic program TURBO-FRODO (A. Roussel and C. Camillau, AFMB, CNRS, Marseilles, France) based on the sequence alignment.

Bacterial expression of CP

A tandem bacterial expression plasmid to simultaneously express Cap1 and Cap2 was constructed in pET-3d (Novagen) (Studier et al., 1990) following the strategy developed by Obinata and colleagues (Soeno et al., 1998). The coding regions of *CAP1* and *CAP2* were amplified by PCR using wt yeast genomic DNA as a template. Oligonucleotides MAW-33 and MAW-34 were used for *CAP1*, and MAW-48 and MAW-36 were used for *CAP2* (Table III). The amplified PCR products were gel purified and subcloned into separate pET-3d vectors; the resulting constructs were verified by DNA sequencing in both directions. The *CAP1* PCR product was digested with AlfIII and BamHI, and then ligated into pET-3d digested with NcoI and BamHI, to make pBJ 1353. The *CAP2* PCR product was digested with BspHI and BamHI, and then ligated into pET-3d digested with NcoI and BamHI, to make pBJ 1354. The tandem expression vector pBJ 1355, allowing simultaneous expression of Cap1p and Cap2p, was then constructed as follows: the DNA sequences corresponding to the T7 promoter region, the ribosome-binding site, the coding sequence of *CAP2*, and the T7 terminator region were amplified by PCR using the forward primer MAW-47 and the reverse primer MAW-46 with pBJ 1354 as template. The amplified product was gel purified, digested with HindIII, and subcloned into pBJ 1353 digested with HindIII. The orientation and sequence of the *CAP2* insert was verified by restriction digest and DNA sequencing of the coding region of *CAP2*.

CP mutants were expressed in bacteria and purified to homogeneity as described previously (Wear et al., 2003), with minor modifications. Yeast actin was purified from strain YJC 0094 (Table V) as described previously (Goode, 2002). Muscle actin was purified and labeled with pyrene as described in Wear et al. (2003). Actin polymerization assays, both kinetic and steady state, were performed as described in Wear et al. (2003). Kinetic rate constants were determined from the time course of seeded actin assembly using Berkeley Madonna, as described previously (Wear et al., 2003).

Yeast CP expression mutants: mutagenesis and strain construction

Plasmids expressing mutant forms of Cap1 or Cap2 from their endogenous promoters (Table IV) were introduced into *cap1*Δ and *cap2*Δ strains (YJC 0390 and YJC 0171, respectively) and into *cap1*Δ *sac6*Δ CEN::*CAP1* and *cap2*Δ *sac6*Δ CEN::*CAP2* strains (YJC 0596 and YJC 0922, respectively).

Mutations of *CAP1*

The template for mutagenesis was a *CAP1* expression plasmid (pBJ 217) containing *CAP1* and its flanking sequences in the *HIS3* CEN plasmid pRS 313 (Sikorski and Hieter, 1989). Cap1Δ258–268: deletion of Cap1 residues Y258–K268. Bases 1970–1971 were changed from AT to GA with oligonucleotides KKT-07 and KKT-08. Cap1Δ251–268: base 1950 was changed from G to A with oligonucleotides KKT-09 and KKT-10. Cap1-Δ239–268: base 1912 was changed from A to T with oligonucleotides KKT-11 and KKT-12. Cap1 R239A: bases 1912–1914 were changed from AGA to GCT with primers KKT-01 and KKT-02. Cap1 R240A: bases 1915–1917 were changed from AGA to GCT with oligonucleotides KKT-03 and KKT-04. Cap1 R240E: bases 1915–1916 were changed from AG to GA with oligonucleotides KKT-13 and KKT-14. Cap1 RR239, 240AA: bases 1912–1917 were changed from AGAAGA to GCTGCT with oligonucleotides KKT-05 and KKT-06. Cap1 W251R: bases 1948–1950 were changed from TGG to CGT with oligonucleotides KKT-17 and KKT-18. Cap1 W251A: bases 1948–1950 were changed from TGG to GCT with oligonucleotides KKT-77 and KKT-78. Cap1 W251F: bases 1949–1950 were changed from GG to TC with oligonucleotides KKT-89 and KKT-90. Cap1 G252R: base 1951 was changed from G to C with oligonucleotides KKT-

Table III. **Sequences of oligonucleotides, listed 5′ to 3′**

Number	Sequence
KKT-01	CAGTTTAAGGCCTTAGCTAGAAGATTACCAGTCACG
KKT-02	CGTGACTGGTAATCTTCTAGCTAAGGCCTTAAACTG
KKT-03	CAGTTTAAGGCCTTAAGAGCTAGATTACCAGTCACG
KKT-04	CGTGACTGGTAATCTAGCTCTTAAGGCCTTAAACTG
KKT-05	CAGTTTAAGGCCTTAGCTGCTAGATTACCAGTCACG
KKT-06	CGTGACTGGTAATCTAGCAGCTAAGGCCTTAAACTG
KKT-07	GCGATTGGCAGTTGAAGATTGGGTAAG
KKT-08	CTTACCCAATCTTCAACTGCCAATCGC
KKT-09	CGAGATCCAAAATTAACTGAGGTAGTGCGATTGGC
KKT-10	GCCAATCGCACTACCTCAGTTAATTTTGGATCTCG
KKT-11	CAGTTTAAGGCCTTATGAAGAAGATTACCAGTC
KKT-12	GACTGGTAATCTTCTTCATAAGGCCTTAAACTG
KKT-13	CAGTTTAAGGCCTTAAGAGAAAGATTACCAGTCACG
KKT-14	CGTGACTGGTAATCTTTCTCTTAAGGCCTTAAACTG
KKT-17	CGAGATCCAAAATTAACCGTGGTAGTGCGATTGGC
KKT-18	GCCAATCGCACTACCACGGTTAATTTTGGATCTCG
KKT-19	CTGGGGTAGTCGTATTGGCAGTTATAG
KKT-20	CTATAACTGCCAATACGACTACCCCAG
KKT-21	GGGGTAGTGCGCGTATTGGCAGTTATAG
KKT-22	CTATAACTGCCAATACGCGCACTACCCC
KKT-27	CCAAACAAAGAACGCATGAATTGCTTCCTCTGCTG
KKT-28	CAGCAGAGGAAGCAATTCATGCGTTCTTTGTTTGG
KKT-29	CTTCCACCAAACAGCTAACGCAGCCATTGC
KKT-30	GCAATGGCTGCGTTAGCTGTTTGGTGGAAG
KKT-75	CAGTTTAAGGCCTTAGAAAGAAGATTACCAGTCACG
KKT-76	CGTGACTGGTAATCTTCTTTCTAAGGCCTTAAACTG
KKT-87	CGAGATCCAAAATTAACGCTGGTAGTGCGATTGGC
KKT-88	GCCAATCGCACTACCAGCGTTAATTTTGGATCTCG
KKT-89	CGAGATCCAAAATTAACTTCGGTAGTGCGATTGGC
KKT-90	GCCAATCGCACTACCGAAGTTAATTTTGGATCTCG
KKT-91	CGAGATCCAAAATTAACTGGCGTAGTGCGATTGGC
KKT-92	GCCAATCGCACTACGCCAGTTAATTTTGGATCTCG
KKT-93	CCAAAATTAACTGGGGTCGTGCGATTGGC
KKT-94	GCCAATCGCACGACCCCAGTTAATTTTGG
KKT-95	GGGGTAGTGCGATTCGTAGTTATAGATTGGG
KKT-96	CCCAATCTATAACTACGAATCGCACTACCCC
KKT-97	GGTAGTGCGATTGGCCGTTATAGATTGGG
KKT-98	CCCAATCTATAACGGCCAATCGCACTACC
KKT-113	GAGATATCTTCCACCAAACATGAAACGCAGCCATTG-CTTCC
KKT-114	GGAAGCAATGGCTGCGTTTCATGTTTGGTGGAAGA-TATCTC
MAW-33	CCACATGTCTAGTAGTAAATTCG
MAW-34	GCGGATCCTCATTTGCCTTCTGCCGC
MAW-36	GCGGATCCCTATAAAGACTGTAAACCTC
MAW-46	CCCAAGCTGGATATCCGGATATAGTTCC
MAW-47	CCCAAGCTTGTCCGGCGTAGAGGATCG
MAW-48	CCAGTCATGAGTGATGCTCAATTCGATC

Table IV. **Mutant CP plasmids**

pBJ#	Other name	Template	Primers
1370	pET-3d/Cap1Δ239–268	pBJ 1355	KKT 11, 12
1371	pET-3d/Cap2Δ264–287	pBJ 1355	KKT 27, 28
1378	pET-3d/Cap1 R239A	pBJ 1355	KKT 1, 2
1385	pET-3d/Cap1Δ239–268/Cap2Δ264–287	pBJ 1355	KKT 11, 12, 27, 28
1398	pET-3d/Cap2Δ261–287	pBJ 1355	KKT 113, 114
1399	pET-3d/Cap1Δ239–268/Cap2Δ261–287	pBJ 1355	KKT 11, 12, 113, 114
1400	pET-3d/Cap1 W251A	pBJ 1355	KKT 77, 78
1401	pBJ 217/Cap1Δ258–268	pBJ 217	KKT 7, 8
1402	pBJ 217/Cap1Δ251–268	pBJ 217	KKT 9, 10
1403	pBJ 217/Cap1Δ239–268	pBJ 217	KKT 11, 12
1404	pBJ 217/R239A	pBJ 217	KKT 1, 2
1405	pBJ 217/R240A	pBJ 217	KKT 3, 4
1406	pBJ 217/R240E	pBJ 217	KKT 13, 14
1407	pBJ 217/RR239, 240AA	pBJ 217	KKT 5, 6
1408	pBJ 217/W251R	pBJ 217	KKT 17, 18
1409	pBJ 217/W251A	pBJ 217	KKT 77, 78
1410	pBJ 217/W251F	pBJ 217	KKT 89, 90
1411	pBJ 217/G252R	pBJ 217	KKT 91, 92
1412	pBJ 217/S253R	pBJ 217	KKT 93, 94
1413	pBJ 217/A254R	pBJ 217	KKT 19, 20
1414	pBJ 217/I255R	pBJ 217	KKT 21, 22
1415	pBJ 217/G256R	pBJ 217	KKT 95, 96
1416	pBJ 217/S257R	pBJ 217	KKT 97, 98
1417	pBJ 119/Cap2Δ264–287	pBJ 119	KKT 27, 28
1418	pBJ 119/Cap2Δ261–287	pBJ 119	KKT 113, 114
1419	pBJ 119/K261A	pBJ 119	KKT 29, 30
1461	pBJ 108/Cap1Δ239–268	pBJ 108	KKT 11, 12

All plasmids were generated for this paper.

91 and KKT-92. Cap1 S253R: base 1954 was changed from A to C with oligonucleotides KKT-93 and KKT-94. Cap1 A254R: bases 1957–1959 were changed from GCG to CGT with oligonucleotides KKT-19 and KKT-20. Cap1 I255R: bases 1960–1961 were changed from AT to CG with oligonucleotides KKT-21 and KKT-22. Cap1 G256R: bases 1963–1965 were changed from GGC to ACG with oligonucleotides KKT-95 and KKT-96. Cap1 S257R: base 1966 was changed from A to C with oligonucleotides KKT-97 and KKT-98.

Mutations of *CAP2*

The template for mutagenesis was a *CAP2* expression plasmid (pBJ 119) containing *CAP2* and its flanking sequences in the *LEU2* CEN plasmid pRS 315 (Sikorski and Hieter, 1989). Cap2Δ264–287: deletion of Cap2 residues A264 through L287. Bases 2650–2652 were changed from AAG to TGA with oligonucleotides KKT-27 and KKT-28. Cap2Δ261–287: bases 2641–2643 were changed from AAG to TGA with oligonucleotides KKT-113 and KKT-114. Cap2 K261A: bases 2641–2643 were changed from AAG to GCT with oligonucleotides KKT-29 and KKT-30.

Electrophoresis and immunoblotting

Whole-yeast cell extracts were subjected to 10% SDS-PAGE and transferred to nitrocellulose. The membrane was blocked with 3% BSA in PBS. Affinity-purified rabbit polyclonal antibodies against Cap1 (R13) and Cap2 (R12) were incubated for 1 h at RT. HRP-conjugated mouse anti–rabbit IgG (Biosource International) was used at 1:40,000. To detect actin, affinity-purified goat anti-yeast actin pAbs (G2) (Karpova et al., 1993) were used, followed by HRP-rabbit anti–goat IgG. An ECL detection kit (Amersham Biosciences) was used. To quantitate total cell content of CP and actin, known quantities of purified yeast CP and actin were loaded on the gel as standards, and the blot was scanned and analyzed by densitometry. The number of cells loaded on the gel was calculated, and mean cell volume was calculated from the major and minor axes of cells from the culture by light microscopy. In two independent experiments, the total actin concentration in the cytoplasm was determined to be 4.4 and 6.1 μM, and the total CP concentration was 0.98 and 1.5 μM.

Fluorescence microscopy

CP and actin were localized with anti-CP antibodies and rhodamine-phalloidin as described previously (Amatruda and Cooper, 1992) in the same strains used to test actin patch polarization. Twinfilin was localized with anti-twinfilin antibodies (Palmgren et al., 2001), provided by Pekka Lappalainen (University of Helsinki, Helsinki, Finland). Digital images were collected on an inverted microscope (model IX70; Olympus) with a PlanApo 100× oil (NA 1.4) objective lens and a cooled CCD camera (Dage-MTI), using NIH Image software on a PowerMac G4.

Assays for null mutant phenotypes

For actin patch polarization, mutated CP genes on plasmids were transfected into strains carrying *cap1* or *cap2* null mutations YJC 0390 or YJC 0171, respectively. Cultures were fixed and stained with rhodamine-phalloidin as described previously (Sizonenko et al., 1996). As a quantitative measure of actin cytoskeleton polarization, we counted the number of actin patches in the mother portion of small-budded cells and defined polarized cells as having <4 patches in the mother. For *sac6* synthetic lethality, mutated CP genes on *URA3* plasmids were shuffled as described previously (Sizonenko et al., 1996). Serial 10-fold dilutions of multiple independent transformants were grown on selective media and were replica plated onto 5-fluoro-orotic acid.

Rhodamine-actin and permeabilized cells

Addition of 0.5 μM rhodamine-labeled actin to permeabilized cells was performed as described previously (Li et al., 1995) with minor modifications. Three strains, YJC 2954 (wt), YJC 2953 (Cap1Δ), and YJC 2967 (Cap1Δ 239–268) were used (Table V). Fluorescence images were collected on an inverted microscope (model IX70; Olympus) using NIH Image software. The fluorescence intensity in specific regions (i.e., whole bud or single patch in bud) was measured using NIH image software. For each dataset, 20 small-budded cells (bud size <1/3 of the mother) from 10 different fields were chosen at random and were measured. Background intensity was measured from an equal-sized area of each field that did not have cells, and was subtracted from the mea-

Table V. **Yeast strains used in this paper**

YJC #	Strain name	Allele	Relevant genotype
0094	None	wt	*MATα rho+ ade2-1 his3-11 15 leu2-3 112 trp1-1 ura3-1*
0171	ΔCap2	*cap2Δ*	*MATa rho+ ade2-1 his3-11 15 leu2-3 112 trp1-1 ura3-1 cap2-Δ1::HIS3*
0390	ΔCap1	*cap1Δ*	*MATa rho+ ade2-1 his3-11 15 leu2-3 112 trp1-1 ura3-1 cap1::TRP1*
0596	ΔSac6		*MATα rho+ sac6::LEU2 cap1::TRP1 ade2-1 his3-11 15 leu2-3 112 trp1-1 ura3-1 [URA3 CAP1]*
0922	ΔSac6		*MATa ade3 ade2 leu2 ura3 trp1 lys2 sac6-69 cap2Δ::HIS3 [ADE3 URA3 CAP2]*
2935	Cap1 R239A	*cap1-10*	*MATa rho+ ade2-1 his3-11 15 leu2-3 112 trp1-1 ura3-1 cap1::TRP1 [HIS3 CAP1]*
2936	Cap1 R240A	*cap1-12*	*MATa rho+ ade2-1 his3-11 15 leu2-3 112 trp1-1 ura3-1 cap1::TRP1 [HIS3 CAP1]*
2953	ΔCap1	*cap1Δ*	*MATa rho+ ade2-1 his3-11 15 leu2-3 112 trp1-1 ura3-1 cap1::TRP1 [HIS3]*
2954	None	wt	*MATa rho+ ade2-1 his3-11 15 leu2-3 112 trp1-1 ura3-1 cap1::TRP1 [HIS3 CAP1]*
2957	Cap1 R240E	*cap1-13*	*MATa rho+ ade2-1 his3-11 15 leu2-3 112 trp1-1 ura3-1 cap1::TRP1 [HIS3 CAP1]*
2958	Cap1 RR239, 240AA	*cap1-14*	*MATa rho+ ade2-1 his3-11 15 leu2-3 112 trp1-1 ura3-1 cap1::TRP1 [HIS3 CAP1]*
2960	Cap1 W251R	*cap1-18*	*MATa rho+ ade2-1 his3-11 15 leu2-3 112 trp1-1 ura3-1 cap1::TRP1 [HIS3 CAP1]*
2961	Cap1 A254R	*cap1-21*	*MATa rho+ ade2-1 his3-11 15 leu2-3 112 trp1-1 ura3-1 cap1::TRP1 [HIS3 CAP1]*
2962	Cap1 I255R	*cap1-22*	*MATa rho+ ade2-1 his3-11 15 leu2-3 112 trp1-1 ura3-1 cap1::TRP1 [HIS3 CAP1]*
2965	Cap1Δ258–268	*cap1-7*	*MATa rho+ ade2-1 his3-11 15 leu2-3 112 trp1-1 ura3-1 cap1::TRP1 [HIS3 CAP1]*
2966	Cap1Δ251–268	*cap1-8*	*MATa rho+ ade2-1 his3-11 15 leu2-3 112 trp1-1 ura3-1 cap1::TRP1 [HIS3 CAP1]*
2967	Cap1Δ239–268	*cap1-9*	*MATa rho+ ade2-1 his3-11 15 leu2-3 112 trp1-1 ura3-1 cap1::TRP1 [HIS3 CAP1]*
2974	Cap2 K261A	*cap2-14*	*MATa rho+ ade2-1 his3-11 15 leu2-3 112 trp1-1 ura3-1 cap2-Δ1::HIS3 [LEU2 CAP2]*
2975	Cap2Δ264–287	*cap2-12*	*MATa rho+ ade2-1 his3-11 15 leu2-3 112 trp1-1 ura3-1 cap2-Δ1::HIS3 [LEU2 CAP2]*
3008	Cap1 R239E	*cap1-11*	*MATa rho+ ade2-1 his3-11 15 leu2-3 112 trp1-1 ura3-1 cap1::TRP1 [HIS3 CAP1]*
3009	Cap1 R241A	*cap1-15*	*MATa rho+ ade2-1 his3-11 15 leu2-3 112 trp1-1 ura3-1 cap1::TRP1 [HIS3 CAP1]*
3014	Cap1 W251A	*cap1-16*	*MATa rho+ ade2-1 his3-11 15 leu2-3 112 trp1-1 ura3-1 cap1::TRP1 [HIS3 CAP1]*
3015	Cap1 W251F	*cap1-17*	*MATa rho+ ade2-1 his3-11 15 leu2-3 112 trp1-1 ura3-1 cap1::TRP1 [HIS3 CAP1]*
3016	Cap1 G252R	*cap1-19*	*MATa rho+ ade2-1 his3-11 15 leu2-3 112 trp1-1 ura3-1 cap1::TRP1 [HIS3 CAP1]*
3017	Cap1 G256r	*cap1-23*	*MATa rho+ ade2-1 his3-11 15 leu2-3 112 trp1-1 ura3-1 cap1::TRP1 [HIS3 CAP1]*
3018	Cap1 S257R	*cap1-24*	*MATa rho+ ade2-1 his3-11 15 leu2-3 112 trp1-1 ura3-1 cap1::TRP1 [HIS3 CAP1]*
3124	Cap1 S253R	*cap1-20*	*MATa rho+ ade2-1 his3-11 15 leu2-3 112 trp1-1 ura3-1 cap1::TRP1 [HIS3 CAP1]*
3459	Cap2Δ261–287	*cap2-13*	*MATa rho+ ade2-1 his3-11 15 leu2-3 112 trp1-1 ura3-1 cap2-Δ1::HIS3 [LEU2 CAP2]*
3481	Sac6-GFP ΔCap1	*cap1Δ*	*MATa SAC6-GFP-HIS3 cap1Δ::KanMX4 his3 leu2 ura3 lys2 met 15*
3596	Sac6-GFP ΔCap1	*cap1Δ*	*MATa SAC6-GFP-HIS3 cap1Δ::KanMX4 his3 leu2 ura3 lys2 met 15 [URA 3]*
3597	Sac6-GFP Cap1	wt	*MATa SAC6-GFP-HIS3 cap1Δ::KanMX4 his3 leu2 ura3 lys2 met 15 [URA3 CAP1]*
3598	Sac6-GFP Cap1Δ239–268	*cap1-9*	*MATa SAC6-GFP-HIS3 cap1Δ::KanMX4 his3 leu2 ura3 lys2 met 15 [URA3 CAP1]*

sured intensity of the buds or patches. The average, SD, and SEM were calculated from the 20 measurements. In some experiments, purified yeast CP was added at 500 nM before the addition of rhodamine-actin. The CP concentration was maintained during the incubation with rhodamine-actin.

F-actin by fluorometry

To determine F-actin levels in wt (YJC 2954), Cap1Δ (YJC 2953), and Cap1Δ239–268 (YJC 2967) strains, a rhodamine-phalloidin binding assay was performed as described previously (Lillie and Brown, 1994; Karpova et al., 1995). In brief, the total protein content of cell aliquots was measured by Bradford assay. Before staining, fixed cells were divided into three equal aliquots. Cells were suspended in 1× PBS containing 0.2% Triton X-100, and were stained with 0.33 μM rhodamine-phalloidin (Molecular Probes, Inc.). In a control aliquot, 300 μM unlabeled phalloidin was also added (Molecular Probes, Inc.). The cells were washed twice with 1× PBS. The bound rhodamine-phalloidin was extracted by incubation in 500 μl methanol. Fluorescence intensity was measured on a spectrofluorometer (QuantaMaster™; Photon Technology International), with excitation at 550 nm and emission at 580 nm. The values obtained for unlabeled phalloidin-containing control samples were subtracted from those obtained for the corresponding samples to correct for nonspecific binding of labeled phalloidin.

F-actin by fluorescence microscopy

Cells were stained with rhodamine-phalloidin as described previously (Sizonenko et al., 1996). Fluorescence microscopy was performed as described above, and intensities of individual cells were measured using NIH Image software. For each dataset, 10 cells in 2–3 different fields chosen at random were measured. Background intensity was measured from an area of each field that did not have cells, and was subtracted.

Actin patch motility

Cortical actin patches were tracked as described previously (Carlsson et al., 2002), using Sac6-GFP. Strain YJC 3481(*SAC6-GFP-HIS3 cap1Δ*) was transfected with a plasmid that expressed nothing (pBJ 82), wt CAP1 (pBJ 108), or Cap1Δ239–268 (pBJ 1461). We confirmed the functionality of the genes by the polarization of the actin patches. Movies of actin patches were collected from a single focal plane near the upper or lower surface of the cell with a microscope system described previously (Castillon et al., 2003). Patch movement was tracked and analyzed with custom software (Carlsson et al., 2002). The software was adapted to Mac OS X by Jill Jeanblanc and Kevin Schmidt in our lab, and is available from the authors.

We are grateful to Jill Jeanblanc and Kevin Schmidt for their work on the tracking software and for their assistance with the actin patch tracking experiments. We thank Dr. Rick Heil-Chapdelaine and Michael Young for technical advice.

This work was supported by grants to J.A. Cooper from the National Institutes of Health (GM47337) and to Y. Maeda from the Special Coordination Funds for Promoting Science and Technology from the Ministry of Education, Culture, Sports, Science and Technology of the Japanese Government. K. Kim was supported by a postdoctoral fellowship from the American Heart Association.

Submitted: 12 August 2003
Accepted: 12 January 2004

References

Adams, A.E.M., J.A. Cooper, and D.G. Drubin. 1993. Unexpected combinations of null mutations in genes encoding the actin cytoskeleton are lethal in yeast.

Mol. Biol. Cell. 4:459–468.

Amatruda, J.F., J.F. Cannon, K. Tatchell, C. Hug, and J.A. Cooper. 1990. Disruption of the actin cytoskeleton in yeast capping protein mutants. *Nature.* 344: 352–354.

Amatruda, J.F., and J.A. Cooper. 1992. Purification, characterization and immunofluorescence localization of *Saccharomyces cerevisiae* capping protein. *J. Cell Biol.* 117:1067–1076.

Amatruda, J.F., D.J. Gattermeir, T.S. Karpova, and J.A. Cooper. 1992. Effects of null mutations and overexpression of capping protein on morphogenesis, actin distribution and polarized secretion in yeast. *J. Cell Biol.* 119:1151–1162.

Balcer, H.I., A.L. Goodman, A.A. Rodal, E. Smith, J. Kugler, J.E. Heuser, and B.L. Goode. 2003. Coordinated regulation of actin filament turnover by a high-molecular-weight Srv2/CAP complex, cofilin, profilin, and Aip1. *Curr. Biol.* 13:2159–2169.

Carlier, M.F., and D. Pantaloni. 1997. Control of actin dynamics in cell motility. *J. Mol. Biol.* 269:459–467.

Carlsson, A.E., A.D. Shah, D. Elking, T.S. Karpova, and J.A. Cooper. 2002. Quantitative analysis of actin patch movement in yeast. *Biophys. J.* 82:2333–2343.

Castillon, G.A., N.R. Adames, C.H. Rosello, H.S. Seidel, M.S. Longtine, J.A. Cooper, and R.A. Heil-Chapdelaine. 2003. Septins have a dual role in controlling mitotic exit in budding yeast. *Curr. Biol.* 13:654–658.

Cooper, J.A., M.C. Hart, T.S. Karpova, and D.A. Schafer. 1999. Capping protein. *In* Guidebook to the Cytoskeletal and Motor Proteins. T. Kreis and R. Vale, editors. Oxford University Press, New York. 62–64.

Goode, B.L. 2002. Purification of yeast actin and actin-associated proteins. *Methods Enzymol.* 351:433–441.

Guex, N., and M.C. Peitsch. 1997. SWISS-MODEL and the Swiss-PdbViewer: An environment for comparative protein modeling. *Electrophoresis.* 18: 2714–2723.

Hug, C., T.M. Miller, M.A. Torres, J.F. Casella, and J.A. Cooper. 1992. Identification and characterization of an actin-binding site of CapZ. *J. Cell Biol.* 116:923–931.

Idrissi, F.Z., B.L. Wolf, and M.I. Geli. 2002. Cofilin, but not profilin, is required for myosin-I-induced actin polymerization and the endocytic uptake in yeast. *Mol. Biol. Cell.* 13:4074–4087.

Karpova, T.S., M.M. Lepetit, and J.A. Cooper. 1993. Mutations that enhance the *cap2* null mutant phenotype in *Saccharomyces cerevisiae* affect the actin cytoskeleton, morphogenesis and pattern of growth. *Genetics.* 135:693–709.

Karpova, T.S., K. Tatchell, and J.A. Cooper. 1995. Actin filaments in yeast are unstable in the absence of capping protein or fimbrin. *J. Cell Biol.* 131:1483–1493.

Lappalainen, P., and D.G. Drubin. 1997. Cofilin promotes rapid actin filament turnover in vivo. *Nature.* 388:78–82.

Li, R., Y. Zheng, and D.G. Drubin. 1995. Regulation of cortical actin cytoskeleton assembly during polarized cell growth in budding yeast. *J. Cell Biol.* 128: 599–615.

Lillie, S.H., and S.S. Brown. 1994. Immunofluorescence localization of the unconventional myosin, Myo2p, and the putative kinesin-related protein, Smy1p, to the same regions of polarized growth in *Saccharomyces cerevisiae. J. Cell Biol.* 125:825–842.

Loisel, T.P., R. Boujemaa, D. Pantaloni, and M.F. Carlier. 1999. Reconstitution of actin-based motility of *Listeria* and *Shigella* using pure proteins. *Nature.* 401: 613–616.

Machesky, L.M., and K.L. Gould. 1999. The Arp2/3 complex: A multifunctional actin organizer. *Curr. Opin. Cell Biol.* 11:117–121.

Mulholland, J., D. Preuss, A. Moon, A. Wong, D. Drubin, and D. Botstein. 1994. Ultrastructure of the yeast actin cytoskeleton and its association with the plasma membrane. *J. Cell Biol.* 125:381–391.

Nefsky, B., and A. Bretscher. 1992. Yeast actin is relatively well behaved. *Eur. J. Biochem.* 206:949–955.

Okada, K., L. Blanchoin, H. Abe, H. Chen, T.D. Pollard, and J.R. Bamburg. 2002. *Xenopus* actin-interacting protein 1 (XAip1) enhances cofilin fragmentation of filaments by capping filament ends. *J. Biol. Chem.* 277:43011–43016.

Palmgren, S., P.J. Ojala, M.A. Wear, J.A. Cooper, and P. Lappalainen. 2001. Interactions with PIP_2, ADP-actin monomers, and capping protein regulate the activity and localization of yeast twinfilin. *J. Cell Biol.* 155:251–260.

Pollard, T.D., and G.G. Borisy. 2003. Cellular motility driven by assembly and disassembly of actin filaments. *Cell.* 112:453–465.

Rodal, A.A., J.W. Tetreault, P. Lappalainen, D.G. Drubin, and D.C. Amberg. 1999. Aip1p interacts with cofilin to disassemble actin filaments. *J. Cell Biol.* 145:1251–1264.

Schafer, D.A., J.A. Waddle, and J.A. Cooper. 1993. Localization of CapZ during myofibrillogenesis in cultured chicken muscle. *Cell Motil. Cytoskeleton.* 25: 317–335.

Schafer, D.A., C. Hug, and J.A. Cooper. 1995. Inhibition of CapZ during myofibrillogenesis alters assembly of actin filaments. *J. Cell Biol.* 128:61–70.

Schafer, D.A., P.B. Jennings, and J.A. Cooper. 1996. Dynamics of capping protein and actin assembly in vitro: Uncapping barbed ends by polyphosphoinositides. *J. Cell Biol.* 135:169–179.

Sikorski, R.S., and P. Hieter. 1989. A system of shuttle vectors and yeast host strains designed for efficient manipulation of DNA in *Saccharomyces cerevisiae. Genetics.* 122:19–27.

Sizonenko, G.I., T.S. Karpova, D.J. Gattermeir, and J.A. Cooper. 1996. Mutational analysis of capping protein function in *Saccharomyces cerevisiae. Mol. Biol. Cell.* 7:1–15.

Soeno, Y., H. Abe, S. Kimura, K. Maruyama, and T. Obinata. 1998. Generation of functional β-actinin (CapZ) in an *E. coli* expression system. *J. Muscle Res. Cell Motil.* 19:639–646.

Studier, F.W., A.H. Rosenberg, J.J. Dunn, and J.W. Dubendorff. 1990. Use of T7 RNA polymerase to direct expression of cloned genes. *Methods Enzymol.* 185:60–89.

Waddle, J.A., J.A. Cooper, and R.H. Waterston. 1993. The alpha and beta subunits of nematode actin capping protein function in yeast. *Mol. Biol. Cell.* 4:907–917.

Wear, M.A., and J.A. Cooper. 2004. Capping protein binding to S100B: implications for the "tentacle" model for capping the actin filament barbed end. *J. Biol. Chem.* In press.

Wear, M.A., A. Yamashita, K. Kim, Y. Maéda, and J.A. Cooper. 2003. How capping protein binds the barbed end of the actin filament. *Curr. Biol.* 13: 1531–1537.

Winter, D., A.V. Podtelejnikov, M. Mann, and R. Li. 1997. The complex containing actin-related proteins Arp2 and Arp3 is required for the motility and integrity of yeast actin patches. *Curr. Biol.* 7:519–529.

Yamashita, A., K. Maéda, and Y. Maéda. 2003. Crystal structure of CapZ: Structural basis for actin filament barbed end capping. *EMBO J.* 22:1529–1538.

Zigmond, S.H., M. Evangelista, C. Boone, C. Yang, A.C. Dar, F. Sicheri, J. Forkey, and M. Pring. 2003. Formin leaky cap allows elongation in the presence of tight capping proteins. *Curr. Biol.* 13:1820–1823.